Available online at www.sciencedirect.com
SCIENCE DIRECT®
Journal of Sound and Vibration 277 (2004) 647–667
JOURNAL OF SOUND AND VIBRATION
www.elsevier.com/locate/jsvi

Definition of a high-frequency threshold for plates and acoustical spaces

G. Rabbiolo[a,*], R.J. Bernhard[b], F.A. Milner[c]

[a] *DaimlerChrysler Corporation, CIMS 483-05-10, 800 Chrysler Drive, Auburn Hills, MI 48326-2757, USA*
[b] *School of Mechanical Engineering, Purdue University, R.W. Herrick Labs, West Lafayette, IN 47907, USA*
[c] *Department of Mathematics, Purdue University, West Lafayette, IN 47907, USA*

Received 21 December 1998; accepted 4 September 2003

Abstract

An extension of the modal overlap factor is introduced that includes ensemble variations and frequency averaging of plates and acoustic spaces. Uniformly and normally distributed variations of geometric and material parameters are considered. Using this modal overlap factor, approximate formulas are derived to identify the limit of predictability for the combined case of damping, ensemble variation, and frequency averaging. The extended modal overlap factor is used to define a high-frequency threshold for plates and acoustical spaces that depends on system parameters and their variations as well as on damping, and the bandwidth of frequency averaging. Monte-Carlo simulations are shown to illustrate and validate the results.

1. Introduction

It is well known that systems produced to have the same nominal characteristics exhibit significant variations of noise, vibration, and harshness (NVH) properties. Such variations are due to many factors, including uncertainties in the dynamical properties of components, assembly variations, and variations caused by varying environmental conditions. As an example, in Ref. [1], transfer functions of nominally identical Isuzu Rodeo trucks are compared which show relatively large variations at high frequencies due to manufacturing variations and temperature variations. The existence of these variations creates a limit of predictability of deterministic models (finite element method (FEM) or boundary element method (BEM)), as discussed in Refs. [2,3]. At high

*Corresponding author. Tel.: +1-248-576-5623; fax: +1-248-576-7936.
E-mail address: gr65@dcx.com (G. Rabbiolo).

0022-460X/$ - see front matter
doi:10.1016/j.jsv.2003.09.015

frequencies, prediction of modes of vibration is not useful since the average behavior shows no modal behavior.

The existence of a limit of predictability also clarifies the issue that arises regarding the utilization of FEM at high frequencies. As the analysis frequency increases, FEM models become more computationally intensive due to the fact that the size of the elements must be very small, on the order of a fraction of the wavelength of the response. It is a common conclusion that analysis at high frequencies is limited by computational power. However, the existence of an intrinsic limit of predictability suggests that analysis at high frequencies should not be done using traditional FEM models regardless of computer resource considerations. Energy finite element methods (EFEM) and statistical energy analysis (SEA) methods have been developed for high-frequency analysis above the limit of predictability. For these methods, average responses are predicted.

For design purposes, it is valuable to be able to quantify the limit of predictability in order to make predictions in the different frequency ranges using appropriate techniques. Traditionally, the limit of predictability, together with the corresponding definition of the frequency bands where statistical methods are appropriate, has been determined based on some statistics of a single implementation of a system.

In Ref. [4], the following qualitative definitions of low, mid, and high frequency are proposed:

- *Low frequency*: The response spectra exhibit strong modal behavior.
- *Mid frequency*: The response spectra exhibit high irregularities, indicating irregular modal density. Boundary conditions, geometry and materials play an important role.
- *High frequency*: The response spectra are ''smooth'', indicating high modal density. Boundary conditions, geometry, and material are not important.

These definitions were developed for a single implementation of a vibro-acoustic system for which the smoothing of the response for increasing frequency is due to modal overlap and damping. A frequency bandwidth of significant response is defined for each natural frequency. This bandwidth increases with the natural frequency. When the frequency of excitation is within this bandwidth, the mode participates significantly in the response of the system. Therefore, as the excitation frequency increases, and consequently, as the modal density (number of modes per unit frequency) increases, the number of modes that overlap increases. The number of modes contributing to the response at a given frequency becomes larger. If enough modes contribute to the response, their sum would appear smooth since peaks and valleys of the modes would, on average, cancel each other.

Schroeder [5] establishes a ''large room'' criterion that defines a frequency above which statistical parameters describing the sound pressure in a room can be estimated. This criterion is based on the count of modal overlap where the damping of the system is introduced through the reverberation time of the room. The ''large room'' criterion is used by Doak [6], to compare his ''spatial irregularity'' theory with the results of Schroeder [7]. Doak shows, both theoretically and experimentally, that one- and two-dimensional modes of the sound field play an important role below the frequency threshold corresponding to the ''large room criterion'' and develops a complementary theory to Schroeder's theory that applies at low frequencies.

The aim of the current work is to provide a *quantitative* definition of low- and high-frequency ranges for cases where the average of ensemble predictions are desired and frequency averaging is appropriate. This definition is consistent with the frequency range characterizations discussed

previously for a single implementation with damping. The mean response over ensembles of plates and acoustic spaces is considered where the ensembles are made up of nominally identical systems for which variations of geometric characteristics and other physical parameters (including the damping coefficient) are allowed, together with the effect of frequency averaging. The frequency threshold is defined by extending the definition of the modal overlap count (modal overlap factor) to include variations of physical parameters across the ensemble, damping, and frequency averaging bandwidth. The derivation takes into account the first two moments (mean and variance) of the physical parameters. The results are checked for both uniform and normal distributions.

The central result of this paper is a formula for a frequency threshold dividing the low- and high-frequency ranges, the limit of predictability. To illustrate and validate the results, Monte-Carlo simulations are done to estimate the average response of plates and acoustic spaces together with the corresponding prediction of the frequency threshold.

2. Modal overlap count

In Ref. [8] a frequency threshold was presented that defines the high- and low-frequency ranges for an ensemble of beams. The ensemble under consideration exhibits variations in all physical parameters. The effects of damping and frequency averaging are also considered.

The main result shown in Ref. [8] is that the mean response over an ensemble of beams reveals a threshold in its behavior at the frequency where the bandwidth $\Delta\omega$, the variation of the natural frequencies due to ensemble variations and variations associated with damping, equals $\delta\omega$, the average distance between adjacent natural frequencies. Above the frequency threshold the modes overlap and the mean response becomes smooth as a function of frequency (high-frequency range).

For the case of the beam, both $\Delta\omega$ and $\delta\omega$ can be written as functions of frequency. Each grows monotonically at different rates. Thus, it is possible to find a unique frequency value (the defined threshold) such that

$$\Delta\omega = \delta\omega. \tag{1}$$

A new variable MO is introduced. It is the average number of modes excited by a pure tone of frequency ω (assuming small damping). A mode is considered excited by a pure tone of frequency ω if ω is in the frequency band $\Delta\omega$ associated with that mode. This definition is the same as the definition of modal overlap factor discussed in the introduction, where the bandwidth corresponding to each mode now depends on the variation of the material properties, β, instead of the damping coefficient. Eq. (1), the threshold condition, can be rewritten as

$$MO = \frac{\Delta\omega}{\delta\omega} = 1.$$

MO depends on the physical variations of an ensemble through the bandwidth $\Delta\omega$ which measures the variation of the natural frequencies.

In the next sub-sections the exact mode count MO is precisely defined as a function of frequency (or wave number) and variations in the physical parameters. MO is found for plates and acoustical spaces. An estimate of MO, $\overline{MO}$, is sought that describes its average behavior. A

general definition of a threshold, involving $\overline{MO}$, will follow. The threshold will be computed using a condition similar to Eq. (1).

3. Multi-dimensional modal overlap count

The modal overlap count is developed first for the general case of a mechanical system (plate, acoustical enclosure, etc.). The dispersion relation is assumed to have the general form

$$\omega = f(\boldsymbol{\beta}, k), \tag{2}$$

where $\boldsymbol{\beta} = (\beta_1, \ldots, \beta_M)$ is a vector of physical parameters that varies in the ensemble. The wave number k is given by

$$k = k(\mathbf{L}, \mathbf{m}) = \sqrt{\sum_{i=1}^{N} \left(\frac{m_i \pi}{L_i} + c_i \right)^2}, \tag{3}$$

where $N = 2, 3$ and $\mathbf{L} = (L_1, \ldots, L_N)$ are the physical dimensions of the system and $\mathbf{m} = (m_1, \ldots, m_N)$ is a multi-index such that the corresponding wave number from Eq. (3) exists for the system considered. The values c_i are constants that depend on the boundary conditions imposed on the system.

For a given multi-index $\mathbf{m}$ the eigenfrequency $\omega = f(\boldsymbol{\beta}, k(\mathbf{L}, \mathbf{m}))$ is regarded as a random variable, a function of the random variables $\boldsymbol{\beta}$ and $\mathbf{L}$, representing the ensemble variations. $\boldsymbol{\beta}$ is a random vector with independent components β_i with mean $\overline{\beta_i}$ and standard deviation $\sigma_{\beta_i} = q_{\beta_i} \overline{\beta_i}$. Analogously, the sizes L_i are independent random variables with mean $\bar{L}_i$ and standard deviation $\sigma_{L_i} = q_{L_i} \bar{L}_i$.

The assumption of this derivation is that the modal overlap count depends only on the first two moments of the random variables involved. In particular, this implies that the results will not depend on the distribution of the variables.

In the following derivation, a measure of the size of the variation of the eigenfrequencies $\Delta\omega$ is established. This is achieved by computing the standard deviation of the variation of each natural frequency and computing the interval of variation by assuming it to be uniformly distributed. To help justify the choice of the uniform distribution for the natural frequencies ω, it must be recalled that the end purpose is the count of the number of modes that overlap. If an interval of variation of the natural frequencies is identified (such as for a uniformly distributed variable) the count of the overlaps should not depend on the exact distributions but only on whether the intervals of variation overlap.

For each given $\mathbf{m}$ the variance of ω is estimated via the formula

$$\sigma_\omega^2 \approx f_{\beta_i}^2(\bar{\boldsymbol{\beta}}, \bar{k}) \sigma_{\beta_i}^2 + f_{L_i}^2(\bar{\boldsymbol{\beta}}, \bar{k}) \sigma_{L_i}^2,$$

where $\bar{k} = k(\bar{\mathbf{L}}, \mathbf{m})$ and the usual summation convention is used. This formula is based on a Taylor expansion of f. Using Eq. (3), the variance can be rewritten as

$$\sigma_\omega^2 = \left\{ \frac{\overline{\beta_i}^2 f_{\beta_i}^2(\bar{\boldsymbol{\beta}}, \bar{k})}{\bar{k}^2} q_{\beta_i}^2 + f_k^2(\bar{\boldsymbol{\beta}}, \bar{k}) \frac{(\bar{k}_i + c_i)^2 \bar{k}_i^2}{\bar{k}^4} q_{L_i}^2 \right\} \bar{k}^2,$$

where $\bar{k}_i = m_i\pi/\bar{L}_i$. As discussed previously, the distribution of ω is assumed uniform. For a random variable uniformly distributed on the interval (a, b) with standard deviation σ, the relation $b - a = 2\sqrt{3}\sigma$ holds and therefore the interval of variation $\Delta\omega$ of ω can be defined as

$$\Delta\omega = 2\sqrt{3}\sigma_\omega = 2\sqrt{3}\left\{\frac{\overline{\beta_i}^2 f_{\beta_i}^2(\bar{\boldsymbol{\beta}}, \bar{k})}{\bar{k}^2} q_{\beta_i}^2 + f_k^2(\bar{\boldsymbol{\beta}}, \bar{k})\frac{(\bar{k}_i + c_i)^2\bar{k}_i^2}{\bar{k}^4} q_{L_i}^2\right\}^{1/2} \bar{k}.$$

For every fixed $\boldsymbol{\beta}$ it is assumed that the function $k \to f(\boldsymbol{\beta}, k)$ is one-to-one and therefore the inverse, $f^{-1}(\boldsymbol{\beta}, \cdot)$, exists. Because of the simple geometry of the wave number space, it is convenient to work with variables in that space. To this end the "change of variable"

$$k \to k^* = f^{-1}(\bar{\boldsymbol{\beta}}, \omega) = f^{-1}(\bar{\boldsymbol{\beta}}, f(\boldsymbol{\beta}, k)), \tag{4}$$

is considered such that k^* depends on $\boldsymbol{\beta}$ and k. As a first order approximation the variation of k^* can be written as

$$\Delta k^* = f_\omega^{-1}(\bar{\boldsymbol{\beta}}, f(\bar{\boldsymbol{\beta}}, \bar{k}))\Delta\omega = \frac{1}{f_k(\bar{\boldsymbol{\beta}}, \bar{k})}\Delta\omega.$$

Therefore, substituting gives

$$\Delta k^* = 2\sqrt{3}\left\{\left[\frac{\overline{\beta_i}}{\bar{k}} f_{\beta_i}^{-1}(\bar{\boldsymbol{\beta}}, f(\bar{\boldsymbol{\beta}}, \bar{k}))\right]^2 q_{\beta_i}^2 + \frac{(\bar{k}_i + c_i)^2\bar{k}_i^2}{\bar{k}^4} q_{L_i}^2\right\}^{1/2} \bar{k}. \tag{5}$$

For each $\mathbf{m}$, relation (5) can be interpreted geometrically (refer to Fig. 1 for the case $N = 2$, $m_1, m_2 \geqslant 1$, and $c_1 = c_2 = 0$). The wave number $\bar{k}$ is represented by the point $P = (m_1\pi/\bar{L}_1 + c_1, \ldots, m_N\pi/\bar{L}_N + c_N)$ and its value is the distance from P to the origin. For variations of $\boldsymbol{\beta}$, and

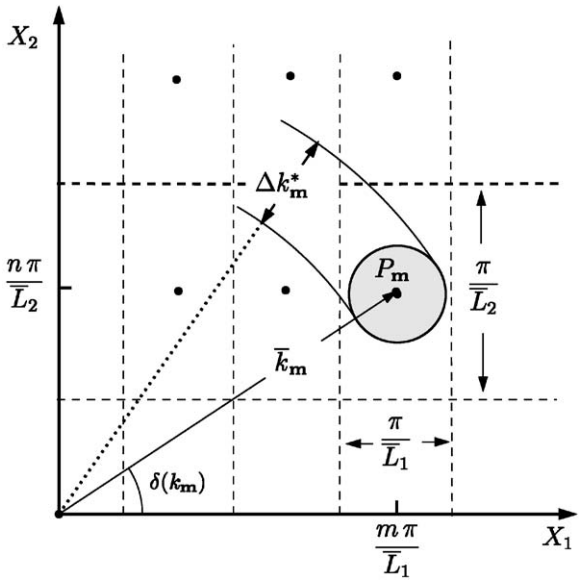

Fig. 1. Representation of eigenfrequencies and their variations.

the sizes **L**, the point corresponding to k^* (see Eq. (4)) spans a region about $\bar{k}$ (in Fig. 1 is the shaded disk centered at P). The Δk^* in Eq. (5) is the size of the interval $I_{\mathbf{m}}$ spanned by k^*.

A precise definition of the modal overlap count MO can be given as

$$MO(k) = \sum_{\mathbf{m}} \chi_{I_{\mathbf{m}}}(k),$$

where χ_A is the indicator function of the set A. $MO(k)$ is the number of intervals $I_{\mathbf{m}}$ that contain k. MO can also be visualized on the plane in Fig. 1 as the number of shaded regions (corresponding to each multi-index **m**) intersected by a circle of radius k centered at the origin. As a function of the q_{β_i}'s and q_{L_i}'s, MO is very irregular with many oscillations. It should be not surprising that there is no simple formula for MO. In the following, an approximation for MO is developed where variations in all of the parameters are considered.

The following notation will be used. For each **m**, let $S_{\mathbf{m}}$ be the parallelepiped centered at $P_{\mathbf{m}}$ with sides of length $\pi/\bar{L}_i$ for $i = 1, \ldots, N$ in the direction of the ith axis. The volume of $S_{\mathbf{m}}$ is $\pi^N/\bar{V}$, where $\bar{V}$ is the average volume of the ensemble of systems (see Fig. 1). Note that the $S_{\mathbf{m}}$'s are non-overlapping and they partition the region containing the points $P_{\mathbf{m}}$. The region D_k is defined as the intersection of the sphere of radius k centered at the origin, with all of the $S_{\mathbf{m}}$'s that correspond to a wave number of the system. Finally, Γ_k denotes the curved portion of the boundary of D_k.

Next, consider the function $T(k)$ defined by

$$T(k) = \sum T_{\mathbf{m}}(k), \tag{6}$$

where $T_{\mathbf{m}}$ is given by

$$T_{\mathbf{m}}(k) = \begin{cases} \Delta k^*_{\mathbf{m}} & \text{if } I_{\mathbf{m}} \text{ lies to the left of } k, \\ \text{Length of the portion of } I_{\mathbf{m}} \text{ on the left of } k & \text{if } I_{\mathbf{m}} \text{ contains } k, \\ 0 & \text{otherwise.} \end{cases}$$

Note that only a finite number of terms in the summation are non-zero. The function $T(k)$ can be loosely visualized in the plane in Fig. 1 as the cumulative sum of the variations $\Delta k^*_{\mathbf{m}}$ corresponding to rectangles $S_{\mathbf{m}}$ lying inside the circle of radius k centered at the origin. If a value k is fixed and a small increment Δk is considered, the quantity $T(k + \Delta k) - T(k)$ is the total length of the portions of the intervals that lie in the interval $(k, k + \Delta k)$. Hence, if Δk is small enough the incremental ratio

$$\frac{T(k + \Delta k) - T(k)}{\Delta k}, \tag{7}$$

is the number of intervals that contain the value k. Therefore, for every k not an endpoint of any $I_{\mathbf{m}}$,

$$MO(k) = T'(k). \tag{8}$$

Thus, $MO(k)$ can be computed from an estimate of $T(k)$. In order to obtain a simple approximation of $T(k)$, a continuous version of Eq. (6) is considered

$$T(k) \approx \int_{D_k} f(\mathbf{x})\, \mathrm{d}\mathbf{x},$$

where the density function $f(\mathbf{x})$ satisfies the condition

$$\int_{S_{\mathbf{m}} \cap D_k} f(\mathbf{x})\,\mathrm{d}\mathbf{x} = T_{\mathbf{m}}(k). \tag{9}$$

In other terms, $f(\mathbf{x})$ can be interpreted as the variation per unit area (density in wave number space) of the natural frequencies at the point $\mathbf{x}$. Therefore, relation (9) suggests the following approximation for f:

$$f(\mathbf{x}) \approx \frac{\bar{V}}{\pi^N} \Delta k^*(\mathbf{x}),$$

where $\Delta k^*(\mathbf{x})$ is the continuous version of Eq. (5),

$$\Delta k^*(\mathbf{x}) = 2\sqrt{3}\left\{\left[\frac{\overline{\beta_i}}{|\mathbf{x}|} f_{\beta_i}^{-1}(\bar{\boldsymbol{\beta}}, f(\bar{\boldsymbol{\beta}}, |\mathbf{x}|))\right]^2 q_{\beta_i}^2 + \frac{(x_i + c_i)^2 x_i^2}{|\mathbf{x}|^4} q_{L_i}^2\right\}^{1/2} |\mathbf{x}|, \tag{10}$$

and $\mathbf{x} = (x_1, \ldots, x_N)$. In view of Eq. (8), an approximation of the incremental ratio (7) is sought with at least first order accuracy in Δk. Considering a small region of thickness Δk about Γ_k, the following approximation is obtained:

$$MO(k) = T'(k) = \lim_{\Delta k \to 0} \frac{T(k + \Delta k) - T(k)}{\Delta k} \approx \frac{\bar{V}}{\pi^N} \int_{\Gamma_k} \Delta k^*(\mathbf{x})\,\mathrm{d}\mathbf{x} \tag{11}$$

(note that here $\mathrm{d}\mathbf{x}$ denotes the measure in dimension $N - 1$). Denoting

$$h(q_\beta, \bar{\boldsymbol{\beta}}, k) = \left[\frac{\overline{\beta_i}}{k} f_{\beta_i}^{-1}(\bar{\boldsymbol{\beta}}, f(\bar{\boldsymbol{\beta}}, k))\right]^2 q_{\beta_i}^2, \tag{12}$$

and changing to circular coordinates by setting $x_i = k f_i(\theta)$ and $\mathrm{d}\mathbf{x} = k^{N-1} J(\theta)\,\mathrm{d}\theta$, so that $|\mathbf{x}| = k$, the following approximation for MO is obtained:

$$MO(k) \approx \frac{2\sqrt{3}\bar{V}k^N}{\pi^N} \int_W \left[h(q_\beta, \bar{\boldsymbol{\beta}}, k) + \left(f_i(\theta) + \frac{c_i}{k}\right)^2 f_i^2(\theta) q_{L_i}^2\right]^{1/2} J(\theta)\,\mathrm{d}\theta, \tag{13}$$

where W is the set of angle coordinates that spans Γ_k.

This is a general formula that applies to systems of any dimension and for any dispersion equation. It is used to approximate MO as a function of the wave number and depends on the ensemble variations accounted for by the relative standard deviations q_{L_i}'s and q_{β_i}'s.

3.1. Frequency averaging and damping

Both frequency averaging over frequency bands and the introduction of damping in the vibration of a system have the effect of smoothing the response. In fact the peaks of the modal responses are wider and lower for frequency averaging and higher damping and the modal overlap count is higher. In this sub-section a prediction of the higher modal overlap count is achieved by augmenting the interval of variation of the eigenfrequencies (Δk^* of the previous sub-section) by an amount that depends on the fraction of octave band on which frequency averaging is considered and on the damping coefficient. This same procedure has been used in Ref. [8] for beams.

For each $\mathbf{m}$, the dependence on frequency averaging and damping is introduced by considering the natural frequencies as random variables of the form

$$\omega_{\mathbf{m}}^{*} = \omega_{\mathbf{m}} + U_{\mathbf{m}} + Z_{\mathbf{m}},$$

where $U_{\mathbf{m}}$ and $Z_{\mathbf{m}}$ are independent random variables accounting for frequency averaging and damping, respectively. An interval of variation is associated with the two variables. We can assume that $U_{\mathbf{m}}$ is distributed uniformly on $[2^{-r/2}\bar{\omega}_{mn}, 2^{r/2}\bar{\omega}_{mn}]$ which is the r-fraction of an octave band on which frequency averaging is performed. $Z_{\mathbf{m}}$ is distributed uniformly on an interval centered at $\bar{\omega}_{\mathbf{m}}$ of length $\eta\bar{\omega}_{mn}$, the half-power bandwidth and η the damping coefficient. In Ref. [8], for beams, the half-power bandwidth was chosen to consider the effect of damping. As discussed previously the choice of uniform distributions for $U_{\mathbf{m}}$ and $Z_{\mathbf{m}}$ may be justified by the fact that only the computation of the number of modal overlaps is considered and the precise distribution of the modes is not assumed important. Since they are uniformly distributed, the variances of $U_{\mathbf{m}}$ and $Z_{\mathbf{m}}$ are given as

$$\sigma_{U_{\mathbf{m}}}^{2} = \frac{\varepsilon^{2}\bar{\omega}_{\mathbf{m}}^{2}}{12}, \quad \sigma_{Z_{\mathbf{m}}}^{2} = \frac{\eta^{2}\bar{\omega}_{\mathbf{m}}^{2}}{12},$$

where $\varepsilon = 2^{r/2} - 2^{-r/2}$.

By the independence assumption $\sigma_{\omega_{\mathbf{m}}^{*}}^{2} = \sigma_{\omega_{\mathbf{m}}}^{2} + \sigma_{U_{\mathbf{m}}}^{2} + \sigma_{Z_{\mathbf{m}}}^{2}$ holds. If the procedure of the previous sub-section is repeated considering ω^{*} instead of ω, relation Eq. (13) is still valid if h in Eq. (12) is replaced by

$$h(q_{\beta}, \varepsilon, \eta, \bar{\boldsymbol{\beta}}, k) = \left[\frac{\overline{\beta_i}}{k} f_{\beta_i}^{-1}(\bar{\boldsymbol{\beta}}, f(\bar{\boldsymbol{\beta}}, k))\right]^{2} q_{\beta_i}^{2} + \left[\frac{1}{k}\frac{f(\bar{\beta}, k)}{f_k(\bar{\beta}, k)}\right]^{2}\frac{\varepsilon^{2}+\eta^{2}}{12}. \tag{14}$$

In the following sections, the general approximation formula (13), together with $h(q_{\beta}, \varepsilon, \eta, \bar{\boldsymbol{\beta}}, k)$ defined above, will be specialized for vibrations of a plate and an acoustical space under specific boundary conditions.

3.2. Plates

A thin, simply supported, rectangular plate of dimensions $L_1 \times L_2$ is considered. For such a plate, the natural frequencies are given by (see Ref. [9])

$$\omega = \boldsymbol{\beta} k^{2}, \quad \text{where } k = \left[\left(\frac{m_1\pi}{L_1}\right)^{2} + \left(\frac{m_2\pi}{L_2}\right)^{2}\right]^{1/2}, \tag{15}$$

for $m_1, m_2 \geqslant 1$, where β depends on various material parameters of the plate. In this case $c_1 = c_2 = 0$ and

$$D_k = \left\{(x, y): x^{2} + y^{2} < k,\ x > \frac{\pi}{2\bar{L}_1}, y > \frac{\pi}{2\bar{L}_2}\right\}.$$

Relation (15) above gives an explicit expression for f in Eq. (2). Using polar co-ordinates, Eqs. (13) and (14) become

$$MO(k) \approx \frac{\sqrt{3}\bar{A}k^{2}}{\pi^{2}} \int_{\delta}^{\pi/2-\delta} \left[\alpha^{2} + 4q_{L_1}^{2}\cos^{4}\theta + 4q_{L_2}^{2}\sin^{4}\theta\right]^{1/2} \mathrm{d}\theta,$$

where $\alpha^2 = q_\beta^2 + (\varepsilon^2 + \eta^2)/12$ and $\delta > 0$ is the angle between the x-axis and the ray from the origin and the point $(k, \pi/2\bar{L}_2)$. By first order approximation of the integrals over $(0, \delta)$ and $(\pi/2 - \delta, \pi/2)$ it is obtained that

$$MO(k) = \frac{\sqrt{3}\bar{A}k^2}{\pi^2} \int_0^{\pi/2} [\alpha^2 + 4q_{L_1}^2 \cos^4\theta + 4q_{L_2}^2 \sin^4\theta]^{1/2}\, \mathrm{d}\theta - \frac{\sqrt{3}\bar{A}k}{2\pi}\left[\frac{(\alpha^2 + 4q_{L_1}^2)^{1/2}}{\bar{L}_2} + \frac{(\alpha^2 + 4q_{L_2}^2)^{1/2}}{\bar{L}_1}\right]. \tag{16}$$

The integral I in Eq. (16) over the variable θ cannot be computed in closed form. However, for $\frac{1}{2} \leqslant q_{L_2}/q_{L_1} \leqslant 2$, an approximation of I can be obtained by splitting the integral over the intervals $[0, \pi/4]$ and $[\pi/4, \pi/2]$. Using the mean value theorem for integrals, it follows that there are values ξ_1 and ξ_2 such that

$$I = \frac{\pi}{4}\{[\alpha^2 + 4q_{L_1}^2 \cos^4\xi_1 + 4q_{L_2}^2 \sin^4\xi_1]^{1/2} + [\alpha^2 + 4q_{L_1}^2 \cos^4\xi_2 + 4q_{L_2}^2 \sin^4\xi_2]^{1/2}\} \approx \frac{\pi}{4}\left[\sqrt{\alpha^2 + 3q_{L_1}^2} + \sqrt{\alpha^2 + 3q_{L_2}^2}\right], \tag{17}$$

where $\xi_1 \in [0, \pi/4]$ and $\xi_2 \in [\pi/4, \pi/2]$. The last approximation is obtained by observing that $q_{L_2}^2 \sin^4\xi_1 \ll q_{L_1}^2 \cos^4\xi_1$ on $[0, \pi/4]$ and $q_{L_2}^2 \cos^4\xi_2 \ll q_{L_1}^2 \sin^4\xi_2$ on $[\pi/4, \pi/2]$ and by considering the approximations $\cos^4(\xi_1) = \sin^4(\xi_2) \approx 3/4$. In Fig. 2 the approximate formula (17) is compared with the value of the integral in Eq. (16) computed numerically. The two graphs correspond to the choices $q_{L_1} = 0.05$, $q_\beta = 0.01$, and $q_{L_1} = 0.01$, $q_\beta = 0.05$. The plots show the value of I versus the ratio q_{L_2}/q_{L_1}. The two functions are well matched.

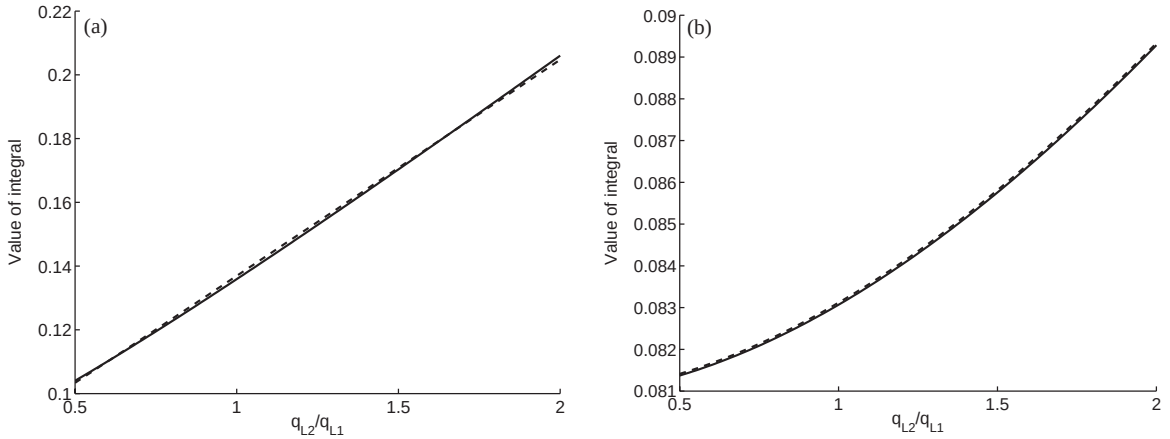

Fig. 2. Comparison of numerical approximation of integral in Eq. (16) and the approximation value from Eq. (17). Parameters values: (a) $q_{L_1} = 0.05$, $q_\beta = 0.01$, (b) $q_{L_1} = 0.01$, $q_\beta = 0.05$. —, numerical integration; - - -, approximation formula.

Substituting Eq. (17) into Eq. (16), the following approximation formula for MO is obtained (for $1/2 \leqslant q_{L_2}/q_{L_1} \leqslant 2$):

$$MO(k) \approx \frac{\sqrt{3}\bar{A}k^2}{4\pi}\left\{\sqrt{\alpha^2 + 3q_{L_1}^2} + \sqrt{\alpha^2 + 3q_{L_2}^2}\right\} - \frac{\sqrt{3}k}{2\pi}\left\{\bar{L}_1\sqrt{\alpha^2 + 4q_{L_1}^2} + \bar{L}_2\sqrt{\alpha^2 + 4q_{L_2}^2}\right\}. \tag{18}$$

Note that for $\alpha = 0$, Eq. (18) reduces to

$$MO(k) \approx \frac{3\bar{A}k^2}{2\pi}\left(\frac{q_{L_1} + q_{L_2}}{2}\right) - \frac{\sqrt{3}k}{\pi}(q_{L_1}\bar{L}_1 + q_{L_2}\bar{L}_2), \tag{19}$$

showing that the variations in dimension are averaged. In many cases $q = q_{L_1} = q_{L_2}$, and Eq. (19) reduces to

$$MO(k) \approx \frac{3\bar{A}qk^2}{2\pi} - \frac{\sqrt{3}qk\bar{P}}{2\pi},$$

where $\bar{P} = 2(\bar{L}_1 + \bar{L}_2)$ is the average perimeter of the plate ensemble.

If $q_{L_1} = q_{L_2} = q_\beta = \varepsilon = 0$, then the modal overlap count due to damping only is obtained as

$$MO(k) \approx \frac{\bar{A}k^2\eta}{4\pi} - \frac{\bar{P}k\eta}{8\pi} = \frac{\eta\omega}{\delta\omega}, \tag{20}$$

where $\delta\omega$ is the average spacing between modes (see Ref. [9]),

$$\delta\omega = \frac{8\pi k\bar{\beta}}{2\bar{A}k - \bar{P}}.$$

The right hand side of Eq. (20) is the ratio of the half-power bandwidth to the average frequency spacing between adjacent eigenfrequencies and can be interpreted as the average number of eigenfrequencies within the half-power bandwidth. This ratio is called the modal overlap factor in the literature. Eq. (18), is a generalization of the concept of modal overlap factor resulting from damping only to the case in which ensemble averaging and frequency averaging are also considered in the determination of modal overlap.

3.3. Acoustic spaces

An acoustic space of dimensions $L_1 \times L_2 \times L_3$ is considered, where the natural frequencies are given by

$$\omega = c_0 k, \quad k = \left[\left(\frac{m_1\pi}{L_1}\right)^2 + \left(\frac{m_2\pi}{L_2}\right)^2 + \left(\frac{m_3\pi}{L_3}\right)^2\right]^{1/2},$$

with $m_1, m_2, m_3 \geqslant 0$ and c_0 is the speed of sound. It holds that $c_1 = c_2 = c_3 = 0$ and the region D_k is then given by

$$D_k = \left\{(x, y, z):\ x^2 + y^2 + z^2 < k^2 \text{ and } x > -\frac{\pi}{2\bar{L}_1}, y > -\frac{\pi}{2\bar{L}_2}, z > -\frac{\pi}{2\bar{L}_3}\right\}.$$

Eqs. (13) and (14) are applied and the following approximation of the modal overlap count is obtained as a function of ω:

$$MO(\omega) \approx \frac{2\sqrt{3}\bar{V}\omega^3}{\bar{c}_0^3\pi^3} \int_W (\alpha^2 + q_{L_1}^2 \sin^4\theta\cos^4\phi + q_{L_2}^2 \sin^4\theta\sin^4\phi + q_{L_3}^2 \cos^4\theta)^{1/2} \sin\theta \, d\theta \, d\phi,$$

where $\alpha^2 = q_{c_0}^2 + (\varepsilon^2 + \eta^2)/12$, and W is the set of angles θ and ϕ that spans Γ_k, the curved portion of the boundary of D_k. $\bar{V} = \bar{L}_1\bar{L}_2\bar{L}_3$ is the volume of the average acoustic space. To compute the integral above, the boundary region Γ_k is split into non-overlapping regions, as shown in Fig. 3. The integrals evaluated on each of these regions and are added up.

The region labeled A, the first octant, corresponds to the square $[0, \pi/2] \times [0, \pi/2]$. The integral on this region represents the major contribution to MO for large values of k. For the other regions, first order approximations of the integrals similar to those used in the case of the plate are considered. Specifically, the thickness of B_1 is approximated as $\pi/(2\bar{L}_3)$ and its contribution to MO is approximated as (cf. Eq. (11))

$$I_{B1} = \frac{\bar{V}}{\pi^3} \int_{B_1} \Delta k^*(\mathbf{x}) \, d\mathbf{x} \approx \frac{\bar{V}}{2\pi^2\bar{L}_3} \int_\gamma \Delta k^*(\mathbf{x}) \, d\mathbf{x},$$

where γ is the arc of radius k in the first quadrant of the space $X_1 - X_2$ (refer to Fig. 3). By setting $x_3 = 0$ in Δk^* as given in Eq. (10), and transforming to polar coordinates to compute the integral in I_{B_1} the following relationship is obtained:

$$I_{B_1} = \frac{\sqrt{3}\bar{L}_1\bar{L}_2\omega^2}{\pi^2\bar{c}_0^2} \int_0^{\pi/2} (\alpha^2 + q_{L_1}^2 \cos^4\theta + q_{L_2}^2 \sin^4\theta)^{1/2} \, d\theta \tag{21}$$

$$\approx \frac{\sqrt{3}\bar{L}_1\bar{L}_2\omega^2}{8\pi\bar{c}_0^2} \left(\sqrt{4\alpha^2 + 3q_{L_1}^2} + \sqrt{4\alpha^2 + 3q_{L_2}^2} \right), \tag{22}$$

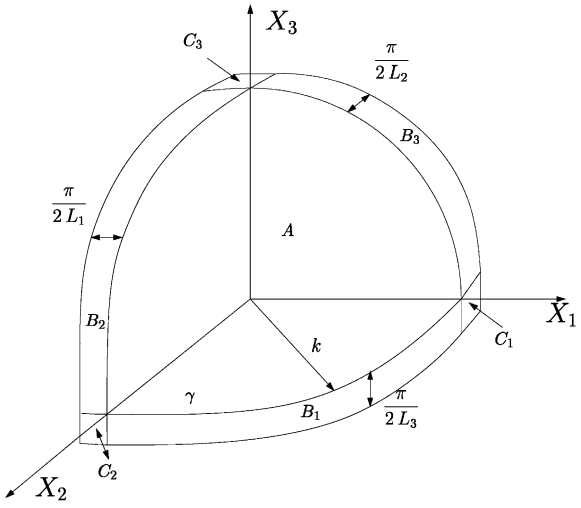

Fig. 3. Subdivision of Γ_k for an acoustic space.

where the approximation of the integral is similar to the one used for the plate. The contributions from B_2 and B_3 are obtained similarly.

Finally, the contribution from the integration on C_1 (refer to Fig. 3) is obtained again from Eq. (10) by approximating the area of C_1 as $\pi^2/(4\bar{L}_2\bar{L}_3)$ and $\Delta k^*(\mathbf{x})$ with its value at $\mathbf{x} = (k, 0, 0)$. The following first order approximation to the contribution of the integral on C_1 to MO is obtained:

$$I_{C_1} = \frac{\sqrt{3}\bar{L}_1\omega}{2\pi\bar{c}_0}\sqrt{\alpha^2 + q_{\bar{L}_1}^2}.$$

Similarly, the integrals on C_2 and C_3 are obtained.

The most general approximation formula for MO is obtained by adding up all the approximation developed above on the surfaces A, B_1, B_2, B_3, C_1, C_2, and C_3.

In the special case in which $q = q_{L_1} = q_{L_2} = q_{L_3}$, the formula simplifies to

$$\begin{aligned} MO(\omega) \approx \frac{2\sqrt{3}\bar{V}\omega^3}{\bar{c}_0^3\pi^3}\int_0^{\pi/2}\int_0^{\pi/2}\Bigg[q_{c_0}^2 + \frac{\varepsilon^2+\eta^2}{2} \\ + q^2(\sin^4\theta\cos^4\phi + \sin^4\theta\sin^4\phi + \cos^4\theta)\Bigg]^{1/2}\sin\theta\,\mathrm{d}\theta\,\mathrm{d}\phi \\ + \frac{\sqrt{3}\bar{S}\omega^2}{8\pi\bar{c}_0^2}\sqrt{4q_{c_0}^2 + \frac{\varepsilon^2+\eta^2}{3} + 3q^2} + \frac{\sqrt{3}\bar{P}\omega}{8\pi\bar{c}_0}\sqrt{q_{c_0}^2 + \frac{\varepsilon^2+\eta^2}{2} + q^2}, \end{aligned} \tag{23}$$

where $\bar{S}$ and $\bar{P}$ are the average surface area and perimeter of the acoustic space, respectively. A closed form expression for the integral in Eq. (23) is not available in the general case and the integral must be evaluated numerically. Because the integrand is smooth, numerical integration is straightforward and many popular algorithms (Newton–Cotes, Gauss–Legendre, etc.) may be used successfully. Moreover, it is reasonable to assume that in the practical use of Eq. (23), tolerances for geometric parameters, damping and frequency averaging coefficients might be fixed for a particular investigation and therefore the integral in Eq. (23) may need to be computed only once.

In special cases a simple expression for Eq. (23) is available. In the case that only geometrical variation is considered ($q_{c_0} = \varepsilon = \eta = 0$), the numerical approximation

$$\int_0^{\pi/2}\int_0^{\pi/2}\sqrt{(\sin^4\theta\cos^4\phi + \sin^4\theta\sin^4\phi + \cos^4\theta)}\sin\theta\,\mathrm{d}\theta\,\mathrm{d}\phi \approx 1.204$$

reduces Eq. (23) to

$$MO(\omega) \approx \frac{4.171\bar{V}\omega^3 q}{\bar{c}_0^3\pi^3} + \frac{3\bar{S}\omega^2 q}{8\pi\bar{c}_0^2} + \frac{\sqrt{3}\bar{P}\omega q}{8\pi\bar{c}_0}.$$

If geometric variability is disregarded ($q = 0$), Eq. (23) simplifies to

$$MO(\omega) \approx \frac{\sqrt{3}\bar{V}\omega^3}{c_0^3\pi^2}\sqrt{q_{c_0}^2 + \frac{\varepsilon^2+\eta^2}{2}} + \frac{\sqrt{3}\bar{S}\omega^2}{8\pi\bar{c}_0^2}\sqrt{4q_{c_0}^2 + \frac{\varepsilon^2+\eta^2}{3}} + \frac{\sqrt{3}\bar{P}\omega}{8\pi\bar{c}_0}\sqrt{q_{c_0}^2 + \frac{\varepsilon^2+\eta^2}{12}}. \tag{24}$$

Finally, the modal overlap count due to damping only ($q_{L_1} = q_{L_2} = q_{L_3} = q_{c_0} = \varepsilon = 0$) is

$$MO(\omega) \approx \frac{\bar{V}\omega^3\eta}{2\pi^2\bar{c}_0^3} + \frac{\bar{S}\omega^2\eta}{8\pi\bar{c}_0^2} + \frac{\bar{P}\omega\eta}{16\pi\bar{c}_0} = \frac{\eta\omega}{\delta\omega}, \tag{25}$$

where $\delta\omega$ is average frequency spacing between natural frequencies given by (see Ref. [9])

$$\frac{16\pi^2\bar{c}_0^3}{8\bar{V}\omega^2 + 2\pi\bar{c}_0\bar{S}\omega + \pi\bar{c}_0^2\bar{P}}.$$

As for the plate, under appropriate assumptions, Eq. (23) reduces to the modal overlap factor due to damping only, where the half-power bandwidth is associated with each mode.

4. Threshold definitions

The approximations of the modal overlap factor MO obtained in the previous section for ensembles of plates and acoustic spaces, are used to define a frequency threshold that separates the low- and high-frequency ranges for multi-dimensional systems. As discussed in Ref. [8] for an ensemble of beams, the onset of the high-frequency range is determined by the lowest frequency at which an overlap of modes is assured. It is possible to characterize the wave number $\tilde{k}$ associated with the frequency threshold for beams in terms of the function $MO(k)$ in the following way:

$$MO(k) \geqslant 1 \quad \text{for all } k > \tilde{k}. \tag{26}$$

For a beam, as mentioned in the introduction, the formula for the threshold presented in Ref. [8] can be written as

$$\overline{MO}(k) = 1, \tag{27}$$

where $\overline{MO}(k)$ is an approximation of $MO(k)$. Therefore, for beams, $\tilde{k}$ defined as in Eq. (26) is actually approximated as the solution of Eq. (27). The distribution of the natural frequencies of a beam is very regular as are the oscillations of $MO(k)$. In particular, below the threshold $\tilde{k}$, the function $MO(k)$ oscillates between the values 0 and 1. Above $\tilde{k}$, it oscillates between 1 and 2, satisfying the general criterion (26), exactly.

Here the criterion in Eq. (26) is generalized to plates and acoustic spaces. The criterion is used to identify the frequency above which the modal overlap becomes substantial, the high-frequency range.

However for general multi-dimensional systems it is impossible to find an exact procedure that computes $\tilde{k}$ from an approximation of MO. For plates and acoustic spaces, the distribution of the natural frequencies is irregular. In particular, $MO(k)$ shows oscillations of amplitude larger

Table 1
Average value of parameters of plate ensemble

x dimension (m)	L_1	0.6
y dimension (m)	L_2	1.67
Thickness (m)	h	0.001
Density (Kg/m^3)	ρ	7850
Young's modulus Pa	E	1.95×10^{11}
Poisson ratio	v	0.3

than 2. The approximations for $MO(k)$ predicted in the previous section follow the average behavior of MO but do not give information about the amplitude of the oscillations. Thus, in general, the solution of Eq. (27) is not expected to give a precise estimate of the threshold $\tilde{k}$ for plates and acoustic spaces.

Instead empirical observations of MO and $\overline{MO}$ functions, based on numerical experiments and a qualitative notion of the high-frequency range, are used to find an approximate $\tilde{k}$ as the solution to

$$\overline{MO}(k) = d,$$

where d is some positive number that will be eventually related to the average amplitude of the oscillations of MO and to the dimension of the system. Observations of the modal overlap factor are done through Monte-Carlo simulations of the average response of plates and acoustical spaces, which will be presented in the next sub-sections.

4.1. Plates

For plates, the averaged squared displacement over all locations for a uniformly distributed unit pressure loading was chosen as the response of interest. The average values chosen for the parameters are shown in Table 1. In these simulations the parameters have been chosen to be uniformly distributed with the relative standard deviations given in the caption.

Fig. 4(a) shows the graph of MO for a plate and the approximation given in Eq. (18), $\overline{MO}$, as a function of frequency (Hz). The plot shows that the threshold $\tilde{k}$ given by Eq. (26) is the wave number corresponding to a frequency of about 220 Hz, while the frequency value corresponding to the solution of Eq. (27) is approximately 100 Hz. This example shows that Eq. (27) cannot be used for plates. For frequencies near 220 Hz, the amplitude of the oscillations is approximately 5 around the average value $\overline{MO}$. Above the value $d = 2.5\ \overline{MO}$ is always greater than 1. Therefore the threshold $\tilde{k}$ is approximated as the solution to

$$\overline{MO}(k) = 2.5. \tag{28}$$

Eq. (28) gives a value of approximately 245 Hz, a much closer estimate of the qualitatively determined value.

Figs. 5(a)–7(a) show MO and $\overline{MO}$ for other plate case studies. The approximation of the threshold with Eq. (28) is very good for all cases. In particular, the plots show that MO is

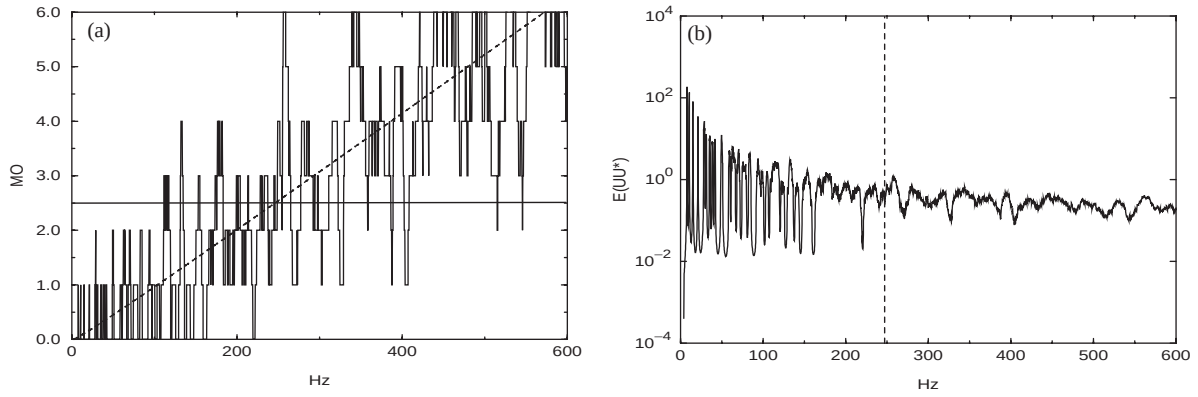

Fig. 4. Simulation of plate ensemble. (a) Modal overlap count MO (solid line) and approximation $\overline{MO}$ (dashed line) with frequency threshold. (b) Average response with frequency threshold. Parameters: $q_{L_1} = q_{L_2} = 0.0058$, $q_\beta = 0$, $\varepsilon = 0$, $\eta = 0.001$. Threshold: 245 Hz.

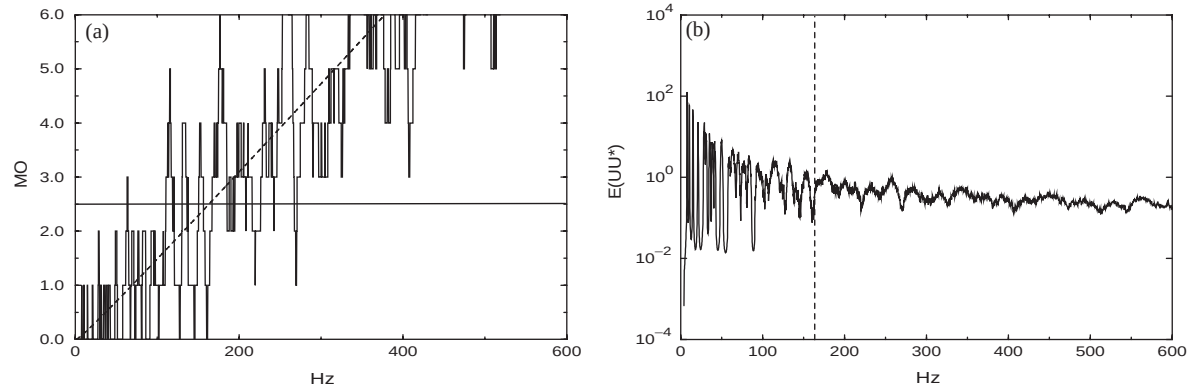

Fig. 5. Simulation of plate ensemble. (a) Modal overlap count MO (solid line) and approximation $\overline{MO}$ (dashed line) with frequency threshold. (b) Average response with frequency threshold. Parameters: $q_{L_1} = q_{L_2} = 0.0058$, $q_\beta = 0.012$, $\varepsilon = 0$, $\eta = 0.001$. Threshold: 163 Hz.

consistently greater than 1 above the frequency corresponding to the wave number solution of Eq. (28).

Figs. 4(b)–7(b) show the average response, as defined above, over an ensemble of 300 plates with variations of the parameters and damping coefficients, corresponding to the plots of MO above them. To compare the plots, the same frequency scaling is used. For each plot, the dashed vertical line is drawn at the frequency value corresponding to the solution of Eq. (28). The vertical lines clearly divide the spectrum into two regions. The mean response has a characteristic behavior that follows the qualitative description of low-frequency behavior on the left-hand side, and high-frequency behavior on the right-hand side. It is interesting to note how the low amplitude responses at low frequencies correspond to the values of frequency for which $MO = 0$; in fact, the frequency bands where $MO = 0$ separate adjacent modes in the low-frequency range. The larger the bands of $MO = 0$ are, the deeper and more well separated are the peaks. In general, peaks and

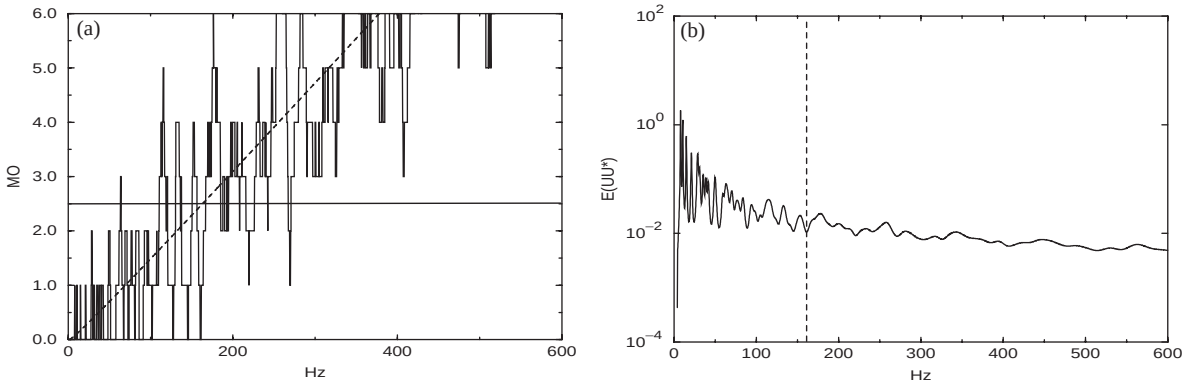

Fig. 6. Simulation of plate ensemble. (a) Modal overlap count MO (solid line) and approximation $\overline{MO}$ (dashed line) with frequency threshold. (b) Average response with frequency threshold. Parameters: $q_{L_1} = q_{L_2} = 0.0058$, $q_\beta = 0$, $\eta = 0.04$. Threshold: 162 Hz.

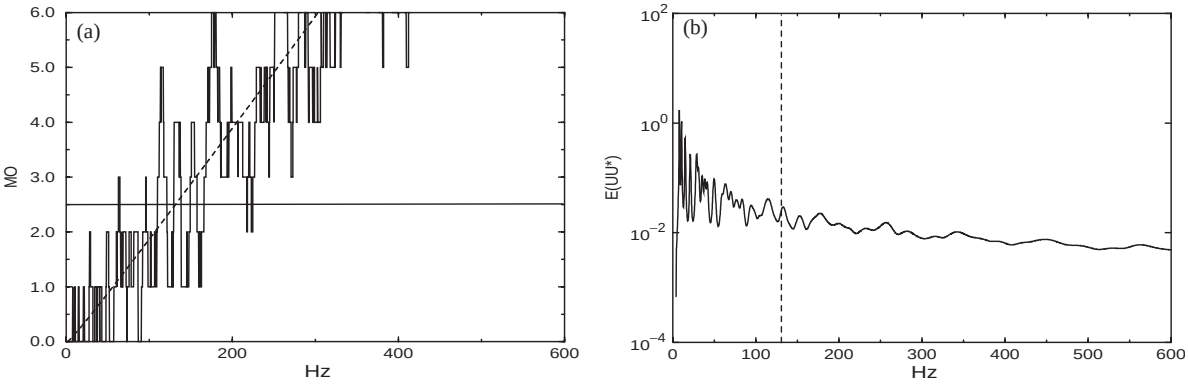

Fig. 7. Simulation of plate ensemble. (a) Modal overlap count MO (solid line) and approximation $\overline{MO}$ (dashed line) with frequency threshold. (b) Average response with frequency threshold. Parameters: $q_{L_1} = q_{L_2} = 0.0058$, $q_\beta = 0.012$, $\eta = 0.04$. Threshold: 131 Hz.

valleys of the graph of MO exactly correspond to peaks and valleys in the response plot. Also, as the modal overlap increases, the oscillations in the response become smoother. In particular, it can be observed that the frequencies of low amplitude responses just above the threshold correspond to the values for which $MO = 1$. These observations suggest that Eq. (28) provides a reasonable and easy to compute implementation of the criterion in Eq. (26). Thus Eq. (28), where $\overline{MO}$ is defined as the right-hand side of Eq. (18), defines a threshold for an ensemble of plates. Nevertheless, the choice of the constant 2.5 is arbitrary and based on a qualitative judgment. Choosing an alternative value for the threshold between values of 1 and 3 is possible and will give somewhat different but consistent results for modal overlap behavior for various ensembles of plates.

As previously discussed, the computation of the modal overlap is based on the first two moments (mean and variance) of the random variables involved and in particular, the derivation

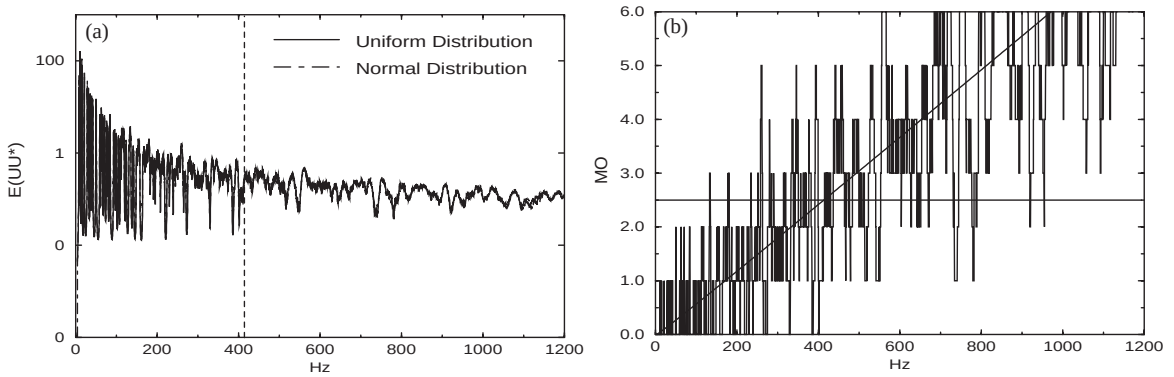

Fig. 8. Simulation of plate ensemble. (a) Modal overlap count MO (solid line) and approximation $\overline{MO}$ (dashed line) with frequency threshold. (b) Average response with frequency threshold. Parameters: $q_x = q_y = 00$, $w = 0.0058$, $f_t = \omega_t/2\pi = 416$ Hz.

does not depend on the distribution of the variables. In order to check if this assumption is plausible, comparison of average responses with parameters uniformly and normally distributed are presented next. In Fig. 8 the average responses of a plate ensemble with uniform and normal distribution of β having the same mean and standard deviation are plotted. The results show the same oscillatory behavior. Also the frequency threshold as indicated by the vertical line is appropriate for both distributions. The function MO and its approximation are also shown. From these simulations it is clear that the definition of a threshold does not depend on the distribution of the parameters.

4.2. Acoustical spaces

All of the observations made for the definition of a frequency threshold for the plate apply also when acoustic spaces are considered. In particular the threshold $\tilde{\omega}$ is defined such that it satisfies the criterion in Eq. (26),

$$MO(\omega) \geqslant 1 \quad \text{for all } \omega > \tilde{\omega}.$$

In Figs. 9–12, Monte-Carlo simulations are shown together with the corresponding plots of MO and $\overline{MO}$. The response of the acoustic spaces was chosen as the mean square acoustic pressure due to a uniformly distributed excitation of unit magnitude, measured at uniformly distributed response points. The values of the average parameters of the acoustic spaces are shown in Table 2. The simulations show the average response over an ensemble of 20 acoustic spaces with uniform variations in the parameters as indicated in the captions. The dashed vertical line corresponds, in each case, to the threshold $\tilde{\omega}$ estimated from the solution of

$$\overline{MO}(\omega) = 3, \tag{29}$$

where $\overline{MO}$ is the right-hand side of Eq. (23). The predicted thresholds are shown to be consistent across the simulations and give a very good prediction of the qualitative transition between the low- and high-frequency ranges. In particular, the effect of damping is shown in Figs. 9 and 10

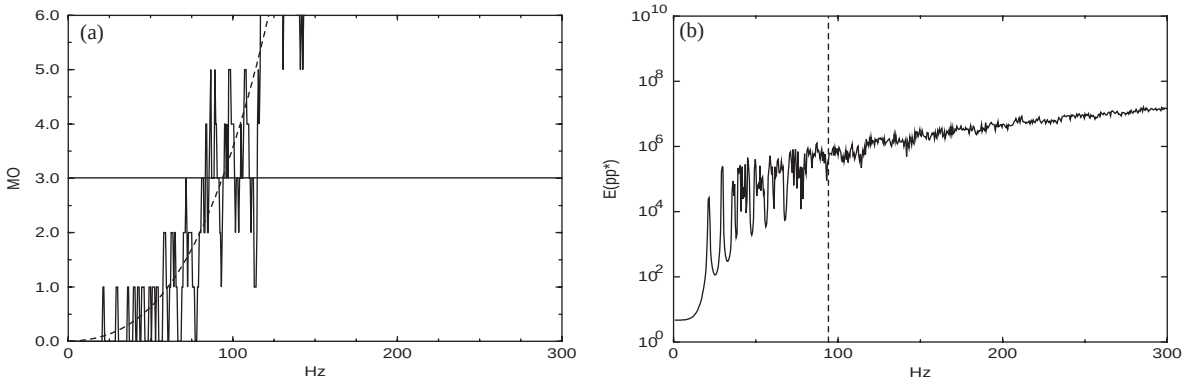

Fig. 9. Simulation of acoustic space ensemble. (a) Modal overlap count MO (solid line) and approximation $\overline{MO}$ (dashed line) with frequency threshold. (b) Average response with frequency threshold. Parameters: $q_{L_1} = q_{L_2} = q_{L_3} = 0.012$, $q_{c_0} = 0.0058$, $\eta = 0.001$. Threshold: 94 Hz.

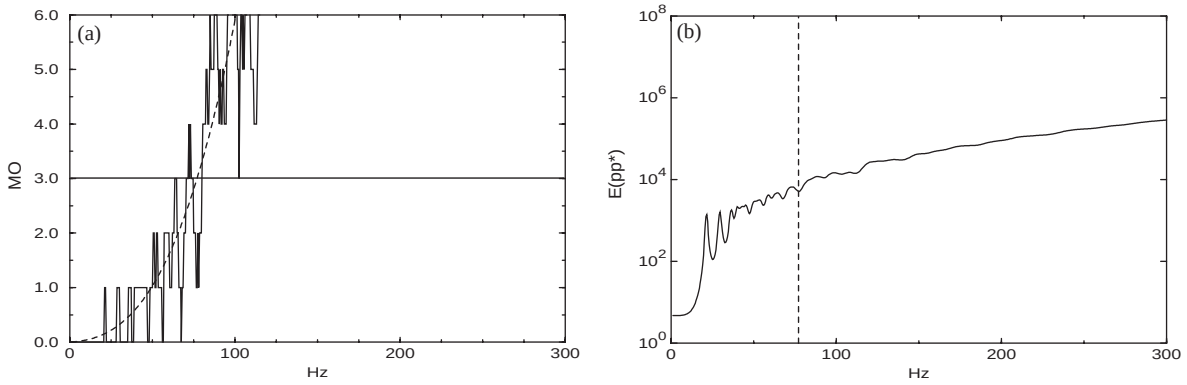

Fig. 10. Simulation of acoustic space ensemble. (a) Modal overlap count MO (solid line) and approximation $\overline{MO}$ (dashed line) with frequency threshold. (b) Average response with frequency threshold. Parameters: $q_{L_1} = q_{L_2} = q_{L_3} = 0.012$, $q_{c_0} = 0.0058$, $\eta = 0.05$. Threshold: 77 Hz.

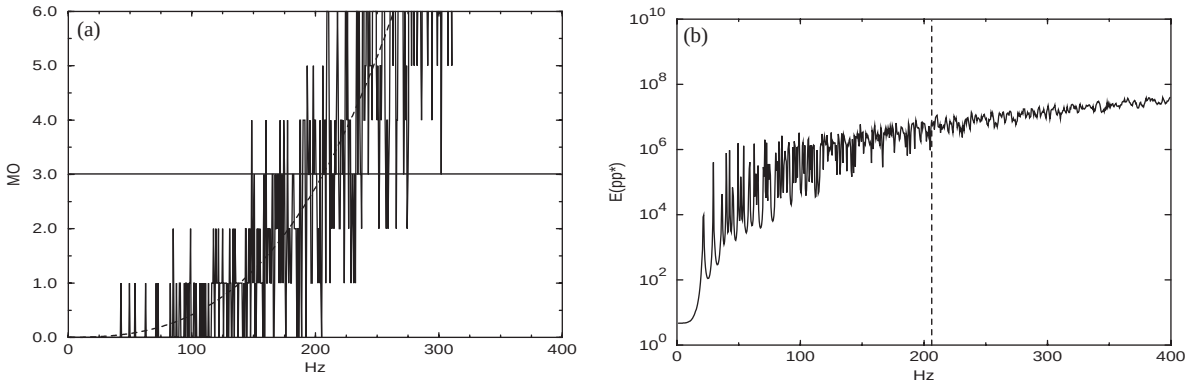

Fig. 11. Simulation of acoustic space ensemble. (a) Modal overlap count MO (solid line) and approximation $\overline{MO}$ (dashed line) with frequency threshold. (b) Average response with frequency threshold. Parameters: $q_{L_1} = q_{L_2} = q_{L_3} = 0.00058$, $q_{c_0} = 0.00012$, $\eta = 0.001$. Threshold: 207 Hz.

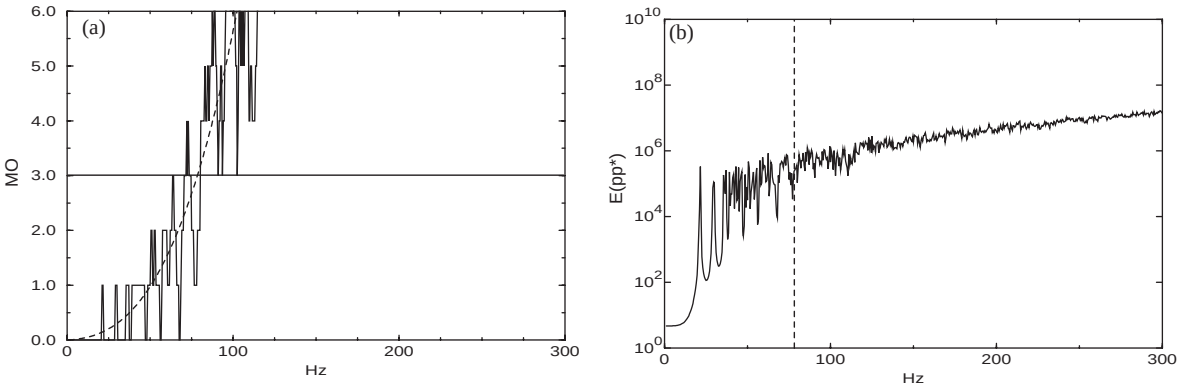

Fig. 12. Simulation of acoustic space ensemble. (a) Modal overlap count MO (solid line) and approximation $\overline{MO}$ (dashed line) with frequency threshold. (b) Average response with frequency threshold. Parameters: $q_{L_1} = q_{L_2} = q_{L_3} = 0.00058$, $q_{c_0} = 0.0017$, $\eta = 0.001$. Threshold: 78 Hz.

Table 2
Average value of parameters of acoustical space ensemble

x dimension (m)	L_1	4.26
y dimension (m)	L_2	8
z dimension (m)	L_3	5.78
density (Kg/m^3)	ρ	1.26
Speed of sound (m/s)	c_0	340

where the average response changes and the threshold reduction are shown with respect to the low damping case. The effect of ensemble averaging is shown by comparing Figs. 9 and 11. The effect of averaging dimensions and averaging on c_0 is illustrated by comparing Figs. 9 and 12. The value 3 in Eq. (29) was determined to be a good threshold by empirical observations as discussed in the case of the plate.

For the damping only case, the frequency threshold is computed by using the estimate of MO in Eq. (25) in condition (29). If the quadratic and linear terms in ω are neglected, the threshold frequency in Hertz is given by

$$f = c_0 \left(\frac{3}{4\pi V \eta} \right)^{1/3}. \tag{30}$$

Using the reverberation time T of the acoustic space given by

$$T = \frac{2.2}{\eta f}.$$

Eq. (30) can be rewritten as

$$f = \sqrt{\frac{3c_0^3}{8.8\pi}} \sqrt{\frac{T}{V}} \approx 2065 \sqrt{\frac{T}{V}}, \tag{31}$$

where $c_0 = 340$. The threshold frequency in Eq. (31) is the Schroeder frequency, the traditional lower limit of the frequency spectrum in which statistical parameters of sound pressure in a room are computed for cases where there are no variations of geometric or material parameters and there is no frequency averaging (see Refs. [10,11]).

5. Conclusions

An extension of the modal overlap factor to include ensemble variations for plates and acoustic spaces has been developed and tested through Monte-Carlo simulations. This extension provides a unifying theory that allows the prediction of the frequency range in which ensembles of plates and acoustic spaces show a "smooth statistical behavior" as consequence of damping, physical parameter variations, and/or frequency averaging. Eq. (13), used with Eq. (14), is the most general formula for the modal overlap factor developed in this paper and can be used for both plates and acoustic enclosures characterized by general dispersion relations and boundary conditions. The assumption of uniformly and normally distributed parameters has been discussed and it has been shown that the threshold is well approximated by considering only the first two moments (mean and variance) of the distribution. Therefore, the threshold formulas written in terms of means and standard deviations can be used for both uniform and normal distributions.

As mentioned in the introduction, in Ref. [7], Schroeder defines a frequency threshold for room acoustics. This theory applies to the frequency range in which the modal overlap factor is greater than 3. This same constant is used in Eq. (29) and gives good prediction of the frequency threshold. The newly defined theory extends the applicability criterion of Schroeder theory to the case in which ensemble variations and frequency averaging are considered.

In this direction, it has been established that for a typical two-dimensional system (plate) the frequency threshold is defined as the value that gives a modal overlap factor of 2.5, and for acoustic space the value 3 is used. Considering the threshold result in Ref. [8] for beams, the threshold is approximated as giving a modal overlap factor of about the space dimension.

The possibility to predict an high-frequency range implies the possibility to choose a priori the appropriate modelling technique in relation to the frequency band being analyzed. Therefore, in the low-frequency range, FEM should be used to give accurate prediction of the characteristic modal behavior, while, in the high-frequency range methods like SEA are appropriate to describe the statistical properties of the system.

References

[1] M.S. Kompella, R.J. Bernhard, Measurements of the statistical variation of structural—acoustic characteristics of automotive vehicles, *Proceedings of the 1993 Noise and Vibration Conference*, 1993, pp. 65–81.

[2] B. Gärdhagen, J. Plunt, Variation of vehicle NVH properties due to component eigenfrequency shifting—basic limits of predictability, *Proceedings of the 1995 Noise and Vibration Conference*, SAE, 1995, pp. 567–576.

[3] R. Bernhard, The limits of predictability due to manufacturing and environmental response of multimode media, *NoiseCon '96*, 1996, pp. 307–312.

[4] J.C. Soize, A. Desanti, Numerical methods in elastoacoustics for low and medium frequency ranges, *La Recherche Aérospatiale, English Ed.* 5 (1992) 25–44.

[5] M. Schroeder, Statistical parameters of the frequency response curve of large rooms, *Journal of Audio Engineering Society* 35 (1987) 299–305.
[6] P. Doak, Fluctuations of the sound pressure level in rooms when the receiver position is varied, *Acustica* 9 (1) (1959) 1–9.
[7] M. Schroeder, Statistical parameters for the frequency response curve of large rooms, *Acustica* 4 (1954) 594–600.
[8] G.R.R.J. Bernhard, F.A. Milner, Vibrations of a beam and related statistical properties, *Mathematical and Computer Modelling* 34 (2001) 657–675.
[9] R.H. Lyon, R.G. DeJong, *Theory and Application of Statistical Energy Analysis*, Butterworth–Heinemann, London, 1995.
[10] M. Schroeder, Frequency-correlation functions of frequency responses in rooms, *The Journal of the Acoustical Society of America* 34 (12) (1962) 1819–1823.
[11] M. Schroeder, The Schroeder frequency revisited, *Journal of the Acoustical Society of America* 99 (1996) 3240–3241.